

Research Articles: Behavioral/Cognitive

Effects of sensorineural hearing loss on cortical synchronization to competing speech during selective attention

<https://doi.org/10.1523/JNEUROSCI.1936-19.2020>

Cite as: J. Neurosci 2020; 10.1523/JNEUROSCI.1936-19.2020

Received: 5 August 2019

Revised: 17 January 2020

Accepted: 30 January 2020

This Early Release article has been peer-reviewed and accepted, but has not been through the composition and copyediting processes. The final version may differ slightly in style or formatting and will contain links to any extended data.

Alerts: Sign up at www.jneurosci.org/alerts to receive customized email alerts when the fully formatted version of this article is published.

Copyright © 2020 Fuglsang et al.

This is an open-access article distributed under the terms of the Creative Commons Attribution 4.0 International license, which permits unrestricted use, distribution and reproduction in any medium provided that the original work is properly attributed.

1 **TITLE:**

2 Effects of sensorineural hearing loss on cortical synchronization to competing speech
3 during selective attention

4

5 **ABBREVIATED TITLE:**

6 Effects of hearing loss on speech processing

7

8 **AUTHORS:**

9 Søren A. Fuglsang^{1,2}, Jonatan Märcher-Rørsted¹, Torsten Dau¹, Jens Hjortkjær^{1,2}

10 ¹ Hearing Systems Section, Department of Health Technology, Technical University of
11 Denmark, Ørsteds Plads, Building 352, DK-2800 Kgs. Lyngby, Denmark

12 ² Danish Research Centre for Magnetic Resonance, Centre for Functional and Diagnostic
13 Imaging and Research, Copenhagen University Hospital Hvidovre, Kettegård Allé 30, DK-
14 2650 Hvidovre, Denmark

15

16 **CORRESPONDING AUTHOR:**

17 Jens Hjortkjær, E-mail address: jhjort@dtu.dk

18 Hearing Systems Section, Department of Health Technology, Technical University of
19 Denmark, Ørsteds Plads, Building 352, 2800 Kgs. Lyngby, Denmark, Tel (+45) 4525395,
20 Fax (+45) 45880577

21

22

23 **AUTHOR CONTRIBUTIONS:**

24 J.H., S.F., T.D. and J.M. designed the experiment, J.M. acquired the data, S.F., J.M. and
25 JH analyzed the data, J.H., S.F. and J.M. wrote the paper, J.H., S.F., T.D. and J.M.
26 corrected the paper and approved the final manuscript

27
28

29 NUMBER OF PAGES: 48
30 NUMBER OF FIGURES: 5
31 NUMBER OF TABLES: 0
32 NUMBER OF WORDS IN INTRODUCTION: 648
33 NUMBER OF WORDS IN DISCUSSION: 1414
34 NUMBER OF WORDS IN ABSTRACT: 247
35 NUMBER OF WORDS IN SIGNIFICANCE STATEMENT: 120

36
37

38 **CONFLICT OF INTEREST:** The authors declare no competing financial interests
39

40 **ACKNOWLEDGMENTS:** This work was supported by the EU H2020-ICT grant number
41 644732 (COCOHA: Cognitive Control of a Hearing Aid) and by the Novo Nordisk
42 Foundation synergy grant NNF17OC0027872 (UHeal).

43

44

45 **Abstract**

46

47 When selectively attending to a speech stream in multi-talker scenarios, low-frequency
48 cortical activity is known to synchronize selectively to fluctuations in the attended speech
49 signal. Older listeners with age-related sensorineural hearing loss (presbycusis) often
50 struggle to understand speech in such situations, even when wearing a hearing aid. Yet, it
51 is unclear whether a peripheral hearing loss degrades the attentional modulation of cortical
52 speech tracking. Here, we used psychoacoustics and electroencephalography (EEG) in
53 male and female human listeners to examine potential effects of hearing loss on EEG
54 correlates of speech envelope synchronization in cortex. Behaviorally, older hearing-
55 impaired (HI) listeners showed degraded speech-in-noise recognition and reduced
56 temporal acuity compared to age-matched normal-hearing (NH) controls. During EEG
57 recordings, we used a selective attention task with two spatially separated simultaneous
58 speech streams where NH and HI listeners both showed high speech recognition
59 performance. Low-frequency (<10 Hz) envelope-entrained EEG responses were enhanced
60 in the HI listeners, both for the attended speech, but also for tone sequences modulated at
61 slow rates (4 Hz) during passive listening. Compared to the attended speech, responses to
62 the ignored stream were found to be reduced in both HI and NH listeners, allowing for the
63 attended target to be classified from single-trial EEG data with similar high accuracy in the
64 two groups. However, despite robust attention-modulated speech entrainment, the HI-
65 listeners rated the competing speech task to be more difficult. These results suggest that
66 speech-in-noise problems experienced by older HI listeners are not necessarily associated
67 with degraded attentional selection.

68

69

70 **Significance statement**

71 People with age-related sensorineural hearing loss often struggle to follow speech in the
72 presence of competing talkers. It is currently unclear whether hearing impairment may
73 impair the ability to use selective attention to suppress distracting speech in situations
74 when the distractor is well segregated from the target. Here, we report amplified envelope-
75 entrained cortical EEG responses to attended speech and to simple tones modulated at
76 speech rates (4 Hz) in listeners with age-related hearing loss. Critically, despite increased
77 self-reported listening difficulties, cortical synchronization to speech mixtures was robustly
78 modulated by selective attention in listeners with hearing loss. This allowed the attended
79 talker to be classified from single-trial EEG responses with high accuracy in both older
80 hearing-impaired listeners and age-matched normal-hearing controls.

81

82 **Introduction**

83

84 One of the most deleterious symptoms of age-related sensorineural hearing loss

85 (presbycusis) is a reduced ability to understand speech in everyday noisy situations. This

86 problem is not always mitigated by amplification of the sounds arriving at the ears, as seen

87 by the fact that many hearing aid users continue to experience substantial difficulties

88 understanding speech in the presence of other sound sources (Kochkin, 2005). Although

89 sensorineural presbycusis is characterized by a degeneration in the cochlea, a range of

90 effects in central auditory processing are likely to influence speech understanding in noisy

91 situations (Peelle and Wingfield, 2016). In young normal-hearing listeners, ongoing low-

92 frequency activity (<10 Hz) in auditory cortex is known to synchronize to slow fluctuations

93 in speech stimuli (Luo and Poeppel, 2007; Aiken and Picton, 2008; Ding and Simon,

94 2012a; Di Liberto et al., 2015). Selectively listening to one speech stream in a speech

95 mixture has been shown to result in an enhanced cortical representation of the attended

96 speech stream compared to the ignored speech (Ding and Simon, 2012b; Golumbic et al.,

97 2013; O'Sullivan et al., 2014). Yet, it is unclear whether presbycusis may interfere with this

98 attentional modulation of cortical synchronization to competing speech signals.

99

100 In situations with competing talkers, speech perception involves at least two distinct

101 processes that could each be hampered by presbycusis (Shinn-Cunningham and Best,

102 2008). First, the ability to perceptually *segregate* the individual sound streams from a

103 sound mixture relies on the encoding of spectro-temporal cues that is often degraded in

104 the impaired system (Grimault et al., 2001). Second, successful speech comprehension

105 additionally involves the ability to *select* relevant speech sources using top-down attention.

106 A failure to segregate speech streams also impairs the ability to attend selectively to

107 particular ones (Dai et al., 2018). Yet, the ability to direct attention to selectively listen to
108 one stream and ignore others may be reduced even in acoustic situations where the
109 competing streams can be segregated.

110

111 Normal aging by itself can lead to declines in both auditory processing and selective
112 attention (Van Gerven and Guerreiro, 2016). Previous studies have reported abnormally
113 enhanced responses to sound envelope fluctuations in the central auditory system with
114 progressing age (Walton et al., 2002; Goossens et al., 2016; Presacco et al., 2016a, 2019;
115 Parthasarathy et al., 2019). Although such cortical hyperactivity occurs in older listeners
116 with clinically normal audiometric thresholds (Presacco et al., 2016a), enhanced envelope
117 responses in cortex also occur with peripheral hearing loss (Millman et al., 2017;
118 Goossens et al., 2018). Enhanced envelope representations may help the detection of
119 sounds in a quiet background but may also degrade the perception of simultaneously
120 fluctuating signals (Moore and Glasberg, 1993; Moore et al., 1995). However, aging is also
121 thought to reduce cortical inhibitory control functions that support the ability to suppress
122 interference from task-irrelevant sensory information (Gazzaley et al., 2005, 2008). Older
123 individuals may thus become more easily distracted by irrelevant information irrespective
124 of their hearing status (Wingfield and Tun, 2001; Andrés et al., 2006). Pressaco et al.
125 (2016b) reported that envelope-entrained responses in older listeners were affected by
126 distracting information to a higher degree than in young listeners. Petersen et al. (2017)
127 reported an enhanced tracking of distractor speech in listeners with presbycusis, but in
128 that study age was correlated with the degree of hearing loss. It is thus unclear to what
129 extent problems with speech understanding in older listeners relate to peripheral deficits
130 and/or to an age-related decline in central attention-related processes.

131

132 To dissociate effects of sensorineural hearing loss from age, the present study compared
133 cortical responses to competing speech streams in older listeners with presbycusis and
134 age-matched normal-hearing controls. We used spatially separated speech stimuli
135 presented at sound levels where speech comprehension remains high, but where speech-
136 listening typically is experienced as more effortful for listeners with hearing loss. We asked
137 whether hearing loss in such situations affects the attention-dependent selective cortical
138 synchronization to attended and ignored speech streams.

139

140

141 **Materials and methods**

142

143

144 ***Participants and audiometry***

145

146 Forty-five subjects participated in this study. It was not possible to obtain scalp EEG data
147 from one subject (normal hearing male, 58 years old), who was therefore excluded from
148 the analysis. Hearing-impaired (HI, N = 22, 9 females, 19 right handed) and normal-
149 hearing (NH, N = 22, 16 females, 18 right handed) subjects between 51 and 76 years of
150 age participated. The HI and NH groups were matched in age ($t(41.98) = -1.62, p =$
151 0.1122 ; NH: mean age 63.0 ± 7.1 ; HI: mean age 66.4 ± 7.0). HI listeners were selected to
152 have a steeply sloping high-frequency hearing loss indicating presbycusis (Bisgaard et al.,
153 2010) (Fig. 2a). For NH listeners, the inclusion criterion was audiometric thresholds within
154 20 dB of normal hearing level (HL) at frequencies up to 2 kHz and within 35 dB HL for
155 frequencies above 2 kHz. One NH subject had a dip in the audiogram at 8 kHz that was 40
156 dB HL on the left ear and 30 dB HL on the right ear. To ensure that subjects with
157 thresholds above the standard clinical threshold of 20 dB HL did not bias our results, we
158 computed the same analyses while excluding NH subjects with thresholds above 20 dB
159 HL. This resulted in a subgroup of 10 NH listeners with ages up to 69 years. To form an
160 age-matched HI subgroup we then similarly selected HI subjects with ages up to 69 years
161 (resulting in a subgroup of 11 HI subjects). This subgroup analysis with a stricter NH
162 criterion produced qualitatively equivalent results in the EEG response data, and the
163 results for the entire group are reported in the following unless stated otherwise. The
164 absolute difference in pure-tone average (PTA; measured at 500 Hz, 1000 Hz, 2000 Hz
165 and 4000 Hz) between ears was less than or equal to 15 dB HL for all subjects.
166 Differences between pure-tone audiometric thresholds across ears were at most 25 dB at
167 individual audiometric frequencies. Bone-conduction thresholds were measured at 0.5, 1

168 and 2 kHz. All subjects had air-bone gaps less than or equal to 10 dB at any audiometric
169 frequency. Tympanometry and otoscopy screening was used to assure normal middle-
170 and outer ear function.

171 All subjects provided written informed consent to participate. The experiment was
172 approved by the Science Ethics Committee for the Capital Region of Denmark (protocol
173 no. H-16036391) and was conducted in accordance with the Declaration of Helsinki.

174

175

176 ***Speech perception in noise***

177 A Danish hearing-in-noise test (DaHINT, Nielsen and Dau, 2009) was used to estimate
178 speech reception thresholds (SRT). Listeners were presented with spoken sentences in
179 speech-shaped stationary noise at equal hearing level (65 dB HL) and asked to repeat the
180 sentences. The stimuli were presented diotically using Sennheiser HD650 headphones in
181 a double-walled sound booth. The level of the speech signal varied adaptively to identify
182 reception thresholds for each subject, indicating the signal-to-noise ratio (SNR) at which
183 the listeners correctly recognize 50% of the presented sentences. Each listener was
184 presented with 3 different lists consisting of 20 sentences, and the SRTs were averaged
185 across lists.

186

187 ***Temporal processing acuity***

188

189 A psychoacoustic tone-in-noise detection test (adapted from Larsby and Arlinger, 1999)
190 was used to assess temporal processing acuity. A pulsating pure tone (500 Hz, 275 ms
191 duration, 2.22 pulses/sec) was presented in different background noise conditions. First,
192 the threshold for tone detection was measured in wide-band noise with a passband
193 corresponding to six equivalent rectangular bandwidths (Moore, 1986) around the target
194 tone frequency. Next, a temporal gap in the noise of 50 ms centered on the tone was

195 introduced. The temporal masking release, i.e. the difference in detection thresholds
196 between the no-gap and gap conditions, was then calculated as a measure of listeners'
197 abilities to utilize temporal fluctuations in the noise masker for improved detection. The
198 noise was presented at a fixed sound pressure level (SPL) of 55 dB and the level of the
199 target tone was varied using a Békésy tracking procedure to identify the thresholds. The
200 subjects performed each condition (no gap, temporal gap) twice for each ear. Subjects
201 also performed a spectral gap detection not included in the analysis. The stimuli were
202 presented using Sennheiser HDA200 headphones in a double-walled sound booth.

203

204 ***Working memory performance***

205

206 Speech perception in noise by older listeners may not only depend on their hearing status
207 but also on cognitive abilities (Akeroyd, 2008) and hearing impairment may itself affect
208 cognitive function (Wingfield and Peelle, 2012). To ensure that the recruited older NH and
209 HI listeners were matched in cognitive abilities, a reversed digit span test was used to
210 measure working memory performance. In the test, listeners were asked to recall a
211 presented sequence of numbers (between 1 and 9) in reverse order. The digit span score
212 was then calculated as the number of items that could be repeated correctly (Blackburn
213 and Benton, 1957). The auditory stimuli were presented via Sennheiser HD650
214 headphones at a comfortable level (70 dB SPL +/-10 dB). The listeners first performed a
215 forward digit span to familiarize them with the procedure.

216

217 ***Self-evaluated hearing disabilities***

218

219 All subjects completed the Speech, Spatial and Qualities of Hearing Scale questionnaire
220 (SSQ, Gatehouse and Noble, 2004). The SSQ questionnaire consists of 49 questions
221 related to self-rated hearing abilities in everyday situations. The questions address hearing

222 in three domains: "Speech" (e.g., comprehending speech and selectively attending to a
223 particular talker in everyday listening situations), "Spatial" (e.g., judging direction, distance
224 and movement of sound sources), "Qualities" (e.g., segregation of sound sources, clarity,
225 and listening effort).

226

227 ***Accounting for reduced audibility***

228

229 The speech stimuli in the DaHINT and EEG experiments were amplified based on the HI
230 listeners' audiometric thresholds to account for reduced audibility. A linear gain was
231 applied at each audiometric frequency according to the 'Cambridge formula' (CamEQ)
232 (Moore and Glasberg, 1998) and was limited to 30 dB gain at a given frequency. The level
233 of the speech stimuli was 65 dB SPL before the frequency-dependent amplification (i.e.,
234 equalization). The tone stimuli used in the EEG experiments were presented at a
235 comfortable listening level per subject.

236

237 ***EEG experiments***

238

239 The EEG experiments were performed in an electrically shielded double-walled sound
240 booth. In all EEG experiments, the subjects were comfortably seated and instructed to
241 fixate their eye-gaze at a cross hair presented on a computer screen. EEG data were
242 recorded using a BioSemi ActiveTwo system with 64-scalp electrodes positioned
243 according to the 10-20 system. Two additional bipolar electrooculography electrodes were
244 mounted above and below the left eye. The EEG data were digitized at a sampling rate of
245 512 Hz. EEG was also measured inside the ear canals in some subjects, but the ear-EEG
246 data were not included in the analysis. The auditory stimuli were presented via ER-3 insert

247 earphones (Etymotic Research). Resting EEG data were also recorded but not considered
248 for analysis.

249
250 ***Tone stimuli***

251
252 Envelope-following responses (EFRs) were recorded from subjects listening passively to
253 tone sequences designed to induce cortical activity in the gamma (40 Hz) and theta (4 Hz)
254 frequency ranges. The stimuli are illustrated in Figure 5a. Two types of stimulation
255 paradigms were used. In both, 1 kHz tone pulses (10 ms Hann-shaped ramps) with an
256 inter-pulse-interval of 25 ms were presented in epochs of 2 s stimulation, alternating with 1
257 s periods of silence. In the first stimulation paradigm, 0.5 s long 40 Hz tone sequences
258 alternated with 0.5 s long silence intervals, resulting in a periodic 4 Hz onset/offset pattern
259 (Fig. 5a top). In the second paradigm, no 4 Hz onset/offset pattern was imposed (Fig. 5a
260 bottom). In each of the two stimulations, 60 3 s long epochs were presented.

261
262
263 Event related potentials (ERPs) during passive listening to 1 kHz pure tones were also
264 recorded. The tone stimuli had a duration of 100 ms and were ramped using a 10 ms long
265 Hann window. The tones were presented at an average inter-tone-interval rate of 1 s that
266 was randomly jittered +/-25 ms. Each subject listened to 180 tone repetitions.

267
268 ***Selective speech attention experiment***

269
270 The main experiment was designed to measure cortical responses to competing speech
271 streams during a selective attention task. EEG data were recorded from subjects
272 selectively listening to one of two simultaneous speech streams or to a single speech
273 stream in quiet. The speech stimuli consisted of two different audiobooks read by a male
274 and a female speaker. Prolonged silent periods in the speech stimuli were truncated to be

275 450 ms long. The audio files were split into ~50 s long trials. The speech streams were
276 spatially separated at +/- 90° using non-individualized head related transfer functions
277 (HRTF) provided by Oreinos and Buchholz (2013). The audio files were low-pass filtered
278 at 12 kHz using a 2nd order Butterworth filter to avoid excessive high-frequency
279 amplification for subjects with low audiometric thresholds. The audio signals of the two
280 talkers were matched in loudness before spatialization according to ITU standard ITU-R
281 BS.1770-1. Loudness matching was used to obtain EEG responses to the two speech
282 streams that were not influenced by systematic differences in sound level between target
283 and masker speech. Subjects were asked to judge the perceived loudness of the two
284 speech streams after the experiment, and all reported that the loudness was perceived to
285 be similar in level.

286

287 Figure 1a presents the trial structure of the selective listening experiment. In ~50 s long
288 trials, the subjects listened to either a single talker or two competing talkers. The
289 experiment consisted of 48 trials. Each subject listened to two blocks of 12 trials with the
290 male speaker as the target, and two blocks of 12 trials with the female speaker as the
291 target. Each block of 12 trials consisted of 4 single-talker trials, and 8 two-talker trials. At
292 the onset of each trial, the subject was instructed to attend to either the male or the female
293 talker. As an additional cue, the target speech stream was switched on ~4 s (jittered
294 between 3 and 5 s) before the interfering speech stream. The EEG data recorded in this
295 period were discarded from analysis. The number of left versus right target trials was
296 balanced across the experiment. After each trial, the subjects were asked to rate how easy
297 or difficult it was to understand the attended speech in that trial on a continuous rating
298 scale marked 'easy' and 'difficult' at the extremes. On average, subjects reported that it

299 was more difficult to follow the male speaker compared to the female speaker. However,
300 the number of trials in which the subjects attended to the male and to the female speaker
301 was balanced within subject. After the rating, listeners were prompted to answer four
302 multiple-choice comprehension questions related to the content of the attended speech
303 stream. The first of the four comprehension questions was also shown before the trial
304 started. Subjects were given feedback on their responses.

305

306 [Insert Figure 1 about here]

307

308 **Data analysis**

309

310 *EEG preprocessing*

311

312 EEG data analyses were performed with Matlab (R2018b, MathWorks) using the Fieldtrip
313 toolbox (20190207; Oostenveld et al., 2011) and the Gramm toolbox for figures (Morel,
314 2016). The digitized EEG data were re-referenced to the average of electrodes TP7 and
315 TP8. EEG data recorded during the selective attention experiment and the EEG data used
316 for extraction of ERPs were low-pass filtered at 30 Hz using a windowed 226th-order linear
317 phase finite impulse response (FIR) filter. The EFR data were low-pass filtered at 60 Hz
318 using a 114th order linear phase FIR filter. Line noise (50 Hz) was removed via DFT-based
319 notch filtering for the ERP and EFR data. The data were then downsampled to 128 Hz for
320 EFR and ERP data and to 64 Hz for the EEG recorded during the selective attention
321 experiment. The ERP and EFR data were subsequently high-pass filtered at 0.1 Hz
322 (VanRullen, 2011; Rousselet, 2012), using a 2112th-order linear phase FIR filter. The EEG
323 data from the attention experiment were high-pass filtered at 0.5 Hz using a 212th-order
324 linear phase FIR filter. The data were segmented into epochs and electroocular (EOG)
325 artefacts were removed (see next paragraph for details). The downsampled and denoised

326 EEG data from the selective attention experiment were finally filtered between 1 Hz and 9
327 Hz. This was done by first applying a 106th-order linear phase FIR high pass filter with a 1
328 Hz cut-off and then low-pass filtering the data with a 94th-order linear phase FIR filter with
329 a 9 Hz cut-off. The data were in all cases shifted to account for the filter delays.

330

331 A joint decorrelation (JD) framework (De Cheveigné and Parra, 2014) was employed to
332 remove EOG artifacts from the EEG speech and ERP data similarly as described in Wong
333 et al. (2018). The mean of each electrode response was first stored and subtracted from
334 the data. Data segments containing EOG artifacts were detected using the Hilbert
335 envelopes of EOG channel responses and responses over three frontal electrodes, Fp1,
336 Fpz and Fp2 and two additional EOG electrodes. The Hilbert envelope of each of these
337 channel responses was extracted after bandpass filtering (passband: 2-15 Hz, 4th order
338 butterworth filter), then z-scored and collapsed into one channel. Time points where the
339 resulting signals exceeded a threshold of four were considered artefactual. The artefactual
340 segments were extended by 0.1 s on both sides (as implemented in Fieldtrip; Oostenveld
341 et al., 2011). The labeled segments were then used to compute an artefact biased
342 covariance matrix. The estimated artefact biased covariance matrix and the covariance
343 matrix estimated from the entire dataset were whitened via principal component analysis.
344 Eigenvectors characterizing the maximum variance differences between the two
345 covariance matrices were then computed (De Cheveigné and Parra, 2014; Wong et al.,
346 2018) using the NoiseTools toolbox (www.audition.ens.fr/adc/NoiseTools). This defines a
347 spatial filter that was then used to regress out EOG artefacts. Eigenvectors with
348 eigenvalues larger than 80% of the maximum eigenvalue were subsequently regressed

349 out from the data (Wong et al., 2018). The mean electrode response that had been
 350 subtracted prior to denoising was added to the denoised data.

351

352 *Extracting ERPs*

353 For the tone response data (ERP/EFR), the mean amplitude of the N1 component (van
 354 Diepen and Mazaheri, 2018) was examined in the time window from 75 to 130 ms post
 355 onset. For this analysis, the EFR data were preprocessed in the same way as for the ERP
 356 data. The data were averaged over a subset of 14 fronto-central electrodes (FC5, FC3,
 357 FC1, FCz, Fz, FC2, FC4, FC6, F5, F3, F1, F2, F4, F6).

358

359 *EFR inter-trial phase coherence*

360 The inter trial phase coherence (ITPC) was computed for EEG responses to EFR stimuli.
 361 To this end, a time-frequency decomposition of each electrode response was performed
 362 by convolving the EEG responses with complex Morlet wavelets with a fixed number of
 363 twelve cycles per wavelet, as implemented in Fieldtrip. No spatial filtering was performed
 364 prior to the analysis. With f_0 representing the passband center frequency of each Morlet
 365 wavelet, we considered an f_0 range between 1 Hz and 50 Hz with a resolution of 0.5 Hz
 366 and a temporal resolution of 2/128 s for visualization purposes. The complex output,
 367 $F_k(f, t, n)$, for trial $k=1, \dots, N$, electrode n , time bin t and center frequency f was then used to
 368 compute the ITPC:

$$\text{ITPC}(f, t, n) = \left| \frac{1}{N} \sum_{k=1}^N \frac{F_k(f, t, n)}{|F_k(f, t, n)|} \right|$$

369 The ITPC ranges between 0 and 1, and indicates the degree of phase consistency of EEG
 370 responses to the EFR stimuli over trials (0 corresponds to no consistency and 1 indicates
 371 full consistency). The ITPC was calculated in non-overlapping windows of 0.5 s to

372 investigate potential changes over the 2 s stimulation period. For the statistical analysis of
373 the EFR data, the average of all scalp electrodes was considered.

374

375 *Speech envelope extraction*

376

377 The speech envelopes of the attended and unattended speech streams were extracted

378 using a simplistic functional model of the auditory periphery. The monaural versions of the

379 audio stimuli were used, i.e. stimuli that had been collapsed via averaging across channel

380 after spatialization. The audio waveforms (digitized at 44.1 kHz) were low-pass filtered at

381 6000 Hz using a 98th-order linear-phase FIR filter, downsampled to 12000 Hz and passed

382 through a 'gammatone' filterbank consisting of 24 4th-order gammatone bandpass filters

383 with center frequencies on an equivalent rectangular bandwidth scale (ranging between

384 100 Hz and 4000 Hz) (Glasberg and Moore, 1990) and 0 dB attenuation at their individual

385 center frequencies. This was based on the implementation available in the Auditory

386 Modeling Toolbox (Søndergaard and Majdak, 2013). The output from each gammatone

387 filter was full-wave rectified and power-law compressed, $|x|^c$, with $c=0.3$ to mimic the

388 compressive response of the inner ear. The output subband envelopes were averaged

389 across gammatone frequency channels to obtain a univariate temporal envelope. The

390 envelope was then low-pass filtered at 256 Hz using a 620th order linear phase FIR filter

391 and resampled to 512 Hz. The envelope was then further low-pass filtered at 30 Hz using

392 a 226th-order linear phase FIR filter and resampled to 64 Hz to match the sampling rate of

393 the EEG data. Finally, the envelope was band-pass filtered as the EEG data between 1 Hz

394 and 9 Hz by first applying a 106th-order FIR high pass filter with a 1 Hz cut-off and then

395 low-pass filtering the data with a 94th-order FIR filter with a 9 Hz cut-off. The filtered data

396 were shifted to adjust for filter delays.

397

398 *Encoding and decoding models*

399

400 Following a number of previous speech-attention studies (e.g. Ding and Simon, 2012b,

401 2013), we considered two complementary analyses of statistical stimulus-response

402 dependencies between the envelope of the attended and unattended speech streams and

403 the EEG responses. We considered both forward regression models (encoding models),

404 and backward regression models (decoding models). The encoding models attempt to

405 predict neural responses to speech stimuli, $R(t, n)$, from the time-lagged speech envelopes

406 $S(t)$

$$\hat{R}(t, n) = \sum_{k=1}^K S(t - \tau_k) w(\tau_k, n),$$

407 where $\hat{R}(t, n)$ is an estimate of the EEG response at a given electrode, $n=1, 2, \dots, N$, and

408 $w(\tau_k, n)$ represent the regression weights that define a temporal response function (TRF).

409 For the encoding analysis, time lags, $\tau_k = \{\tau_1, \tau_2, \dots, \tau_K\}$, ranging between 0 ms and 500 ms

410 post-stimulus were considered.

411 The backward decoding model, on the other hand, integrates information over all EEG

412 electrodes and all time lags to reconstruct the speech envelope:

$$\hat{S}(t) = \sum_{n=1}^N \sum_{k=1}^K R(t - \tau_k, n) w(\tau_k, n).$$

413 For the decoding analysis, we considered time-lags $\tau_k = \{\tau_1, \tau_2, \dots, \tau_K\}$, ranging between -500

414 ms and 0 ms post-stimulus. For both encoding and decoding models, we included data

415 from 6 s after trial onset (i.e. after the onset of any masking stimulus) to 43 s after trial

416 onset.

417 The weights of the linear regression models were estimated via ridge regression. Let X be

418 a standardized matrix and let $X = \mathbf{U}\mathbf{D}\mathbf{V}^T$ be the singular-value decomposition of X .

419 Similarly, let Y be a vector with zero mean and unit standard deviation. The linear

420 regression model can now be formulated as:

$$\hat{Y} = Xw,$$

421 where \hat{Y} is an estimate of Y . The Ridge regression estimator then takes the form:

$$w = \operatorname{argmin}_w [(Y - Xw)^T(Y - Xw) + \lambda w^T w] = (X^T X + \lambda I)^{-1} X^T Y = V(D^2 + \lambda I)^{-1} D U^T Y.$$

422 In the case of a forward encoding model, X is a matrix containing the speech envelope,
 423 $S(t)$, at multiple time lags and Y is the EEG response at a given channel. In this case,
 424 separate Ridge parameters are estimated for each electrode, each subject and each
 425 experimental condition. In the case of a backward model, X is a matrix containing the
 426 multi-channel and time-lagged EEG response and Y is the speech envelope.

427 To assess the predictive performance of each model we used a nested cross-validation
 428 procedure. The nested cross-validation procedure consisted of an outer 10-fold cross-
 429 validation loop and an inner 5-fold cross-validation loop. The data were split 10 times into
 430 a training set and a test set, and for each split we further divided the training data
 431 randomly into 5 parts to optimize the Ridge λ parameter. In this way, the Ridge parameter
 432 was tuned on the training set and the generalization error was evaluated on the held-out
 433 test set. During model fitting and evaluation, the data were standardized to the empirical
 434 mean and unit standard deviation of the data used for model fitting. The prediction
 435 accuracy was indexed by the Pearson's correlation coefficient between the model
 436 prediction \hat{Y} and the target data, Y . Pearson's correlation coefficient was chosen as the
 437 metric since it ranges between -1 and +1 and is invariant to scaling and shift errors in the
 438 predictions. The prediction accuracy was estimated as the average over the 10 initial
 439 splits. The performance of the stimulus-response models was in all cases evaluated on
 440 data from trials that had not been used for model fitting or parameter tuning.

441 For the statistical analysis of the results from the encoding analyses, we averaged the
 442 encoding accuracies over the same subset of fronto-central electrodes as in the ERP

443 analysis. The noise floor was estimated as in Wong et al. (2018) by phase scrambling
444 target regressors (Prichard and Theiler, 1994). The noise floor was estimated based on
445 aggregated surrogate data from all subjects and all stimulus-response models (i.e.,
446 attended single-talker, attended two-talker and unattended two-talker).

447

448 Our stimulus-response analyses were based on envelopes extracted via auditory models
449 that assume a healthy auditory system. Since hearing loss may change this
450 representation, we conducted control analyses to understand whether our results were
451 influenced by these assumptions. First, hearing loss may be associated with a reduced
452 compressive response of the inner ear. To understand whether the results are influenced
453 by the amount of compression assumed by our model, we performed the same analyses
454 with joint encoding models trained on speech envelopes that were compressed with a
455 range of compression factors ($c = \{0.1, 0.2, 0.3, \dots, 1\}$). This analysis yielded equivalent
456 results indicating that the choice of compressive factor ($c=0.3$) did not introduce a group-
457 level bias in model prediction accuracies. Second, hearing loss may distort the coding of
458 envelope modulations in a frequency-specific way that is not captured by a model
459 assuming a broad-band envelope representation. We therefore performed the encoding
460 analyses with models trained on frequency-decomposed cochleograms of the binaural
461 stimuli. We used a gammatone filterbank consisting of 34 filters with center frequencies on
462 an equivalent rectangular bandwidth scale ranging from 100 Hz and to 12000 Hz, allowing
463 the encoding models to capture modulations in high frequency critical-bands. This analysis
464 also yielded very similar results, suggesting that the univariate envelope extraction
465 procedure did not introduce biases in the group-level comparisons. Finally, we checked
466 whether the amplification of the audio stimuli would influence the results by performing the

467 stimulus-response analyses both with and without the CamEQ equalization. This also
468 yielded highly similar results. The results from the analyses obtained with the non-
469 equalized stimuli are reported in the following.

470

471 The ability to decode attention, i.e. to discriminate between attended and unattended
472 speech envelopes from the EEG data, provides a complimentary measure of how robustly
473 the envelope-entrained responses are modulated by attention. We therefore additionally
474 trained backward models on the single-talker data and then used the models to
475 reconstruct the speech envelopes of the attended talker in the remaining two-talker EEG
476 data. To ensure an unbiased decoding, the Ridge parameter and EOG denoising filters
477 were fitted based on the single-talker data. For testing, we considered non-overlapping
478 EEG decoding segments of 10 s duration (taking into account the 0.5 s long kernel of the
479 stimulus reconstruction models) shifted by 15 s long time shifts. To evaluate the attention
480 decoding accuracy, we computed the Pearson's correlation coefficient between the
481 reconstructed envelopes and the envelopes of the attended (r_{attended}) and unattended
482 ($r_{\text{unattended}}$) speech streams (O'Sullivan et al., 2014). We considered a classification to be
483 correct whenever the neural reconstruction was more correlated with the envelope of the
484 actual attended speech stream than with the envelope of the unattended speech stream
485 (i.e., $r_{\text{attended}} > r_{\text{unattended}}$). Chance-level classification was assumed to follow a binomial
486 distribution.

487

488 **Statistical analysis**

489 Repeated measures analyses of variances (ANOVAs) were used to analyze the results
491 from the stimulus-response analyses in the single-talker and the two-talker conditions for

492 attended speech at the group level. Repeated measures ANOVAs were also used for
493 group-level analysis of the average ITPC results in short time windows. Welch's t-tests
494 were used to compare psychophysical results (speech-in-noise scores, SSQ ratings, FT-
495 test scores and digit span scores) and EEG stimulus-response results between the NH
496 and HI listener groups. Pearson's correlation coefficients were transformed using the
497 Fisher Z-transformation prior to statistical analyses. Classification scores, speech
498 comprehension scores, ITPC values and difficulty ratings were arcsin transformed prior to
499 statistical analyses. When appropriate, we used the false discovery rate (Benjamini and
500 Hochberg, 1995) to correct for multiple comparisons. All statistical tests were conducted
501 using R version 3.6.0 (2019-04-26).

502

503 ***Data and code accessibility***

504 All data are publicly available at <http://doi.org/10.5281/zenodo.3618205>. Code is available at
505 <https://gitlab.com/sfugl/snhl>.

506

507

508

509 **Results**

510

511

512 ***Behavioral hearing tests***

513

514 Figure 2 summarizes the data of the behavioral hearing tests. For speech-in-noise

515 perception (Fig. 2b), HI listeners showed significantly higher sentence reception thresholds

516 compared to the age-matched NH controls (DaHINT test: $t(35.78) = -3.49$, $p = 0.0013$).

517 This reduced speech-in-noise performance was observed despite the fact that the speech

518 stimuli were amplified to account for reduced audibility in the HI listeners. Noticeably, the

519 50% speech reception thresholds were negative also for most HI listeners and below

520 SNRs typically encountered in everyday environments (Billings and Madsen, 2018).

521 HI listeners also exhibited a reduced temporal masking release compared to the NH

522 listeners ($t(32.74) = 5.53$, $p < 0.0001$; Fig. 2d) suggesting a degraded temporal processing

523 acuity. In the questionnaire data, HI listeners reported greater difficulties with speech

524 listening in everyday listening situations when wearing their own hearing aid. The different

525 SSQ ratings related to spatial hearing, speech perception and sound quality were

526 correlated (Spearman's rank correlations: $r(\text{SSQ speech, SSQ spatial}) = 0.79$, $r(\text{SSQ}$

527 $\text{speech, SSQ quality}) = 0.82$, $r(\text{SSQ spatial, SSQ quality}) = 0.86$). The SSQ ratings

528 averaged across the three response categories were significantly lower for the HI group

529 compared to the NH listeners ($t(33.10) = 6.49$, $p < 0.0001$, Fig. 2c). Finally, the reversed

530 digit span test confirmed similar working memory performance in the age-matched normal-

531 hearing and hearing-impaired listeners ($t(37.85) = 0.68$, $p = 0.5016$; Fig. 2e).

532

533

[Insert Figure 2 about here]

534

535

536 ***Behavioral results from selective attention experiment***

537

538 During the EEG speech listening experiments, listeners responded to speech

539 comprehension questions and rated speech-listening difficulty. These behavioral results

540 are shown in Figure 1b. Both normal-hearing and hearing-impaired listeners showed

541 accurate speech comprehension, both in the single-talker condition and in the condition

542 with two competing talkers. A repeated measures ANOVA showed no significant effect of

543 hearing impairment on speech comprehension scores ($F(1,42) = 1.31, p = 0.2598$), but a

544 main effect of talker condition (single vs two talkers, $F(1,42) = 8.42, p = 0.0059$). Although

545 the two listener groups answered the comprehension questions with high accuracy, the HI

546 listeners rated the competing speech listening task to be significantly more difficult

547 compared to the NH listeners and compared to the single-talker condition (main effect of

548 hearing impairment on difficulty ratings $F(1,42) = 10.5, p = 0.0023$; Fig. 1b, left).

549

550 ***Speech envelope entrainment during selective attention***

551 In the speech attention experiments, normal-hearing and hearing-impaired subjects

552 listened to speech in quiet or to speech masked by a competing talker. To investigate EEG

553 correlates of cortical speech envelope entrainment in the two groups, we used forward and

554 backward stimulus-response models. Forward model prediction accuracies, i.e. the

555 correlation between the low-frequency EEG response and the response predicted by the

556 envelope model, are shown in Figure 3. A repeated-measures ANOVA was used to test

557 the effect of hearing impairment on the speech envelope entrainment as measured by the

558 EEG prediction accuracies of the forward model on fronto-central electrodes. Envelope

559 entrainment to the target speech was enhanced in HI listeners compared to NH controls in

560 both the single-talker and in the two-talker listening conditions. Main effects of hearing

561 status (NH vs HI, $F(1,42) = 7.57, p = 0.0087$) and stimulus condition (single-talker vs two-
562 talker, $F(1,42) = 54.23, p < 0.0001$) were found, but no significant interaction between the
563 two ($F(1,42) = 0.42, p = 0.5195$). No effect of hearing status on the entrainment for the
564 unattended speech was found ($t(42.00) = -0.10, p = 0.9204$).

565

566 As a complimentary measure of speech envelope entrainment, the backward model
567 reconstructs the envelope of attended and unattended speech streams from a weighted
568 response of all EEG electrodes. Analysis of the envelope reconstruction accuracies
569 between groups again showed a main effect of hearing status ($F(1,42) = 13.76, p =$
570 0.0006), and stimulus condition (single-talker vs two-talker) ($F(1,42) = 56.03, p < 0.0001$),
571 indicating again an enhanced envelope representation in the HI listener group. No effect of
572 hearing impairment was observed on the reconstruction accuracies for the unattended
573 speech ($t(39.69) = -1.34, p = 0.1885$).

574

575 [Insert Figure 3 about here]

576

577 Both analyses suggested a robust differential entrainment to the attended and unattended
578 speech signals in both groups, similar to what has been previously reported for NH
579 listeners (e.g. Ding and Simon, 2012a; O'Sullivan et al., 2014). We next investigated the
580 degree to which this differential response could be used to decode the attentional focus
581 (the attended talker) from single-trial EEG responses. Here, we used the backward models
582 trained on data from single-talker trials. The models were then used to identify the
583 attended target in the EEG responses to the two-talker mixtures. Accurate attention
584 classification here does not by itself necessarily suggest that r_{attended} is high, but only that it
585 is higher than $r_{\text{unattended}}$. Fig. 4 shows the results of the attention decoding analysis. We

586 found that the reconstructed envelopes reliably discriminated between attended and
587 unattended speech in both groups of listeners. The mean classification accuracy for 10 s
588 long EEG segments was 83.7 % for the HI listeners and 79.3 % for the NH listeners and
589 we found no effect of hearing loss on the attention classification accuracies ($t(41.40) = -$
590 1.64 , $p = 0.1077$). Restricting the audiometric criterion for normal hearing (<20 dB HL, see
591 Methods) yielded a significant effect of hearing loss on classification accuracy ($t(16.91) = -$
592 3.074 , $p = 0.0069$).

593

594 The lack of an effect of hearing loss on attention classification in the main analysis may
595 seem puzzling given the enhanced envelope responses for attended speech in the HI
596 listeners. For attention classification, however, we used models trained on single-talker
597 data to predict the envelope of both the target and the non-target speech. This was
598 motivated by the fact that a classification system, e.g. in an EEG-controlled BCI, typically
599 does not know in advance the ‘ground truth’ of which speakers are attended. In the
600 envelope-entrainment analysis (Fig. 3), on the other hand, separate response functions
601 were estimated for attended and unattended speech. The rationale for this was that
602 response functions for attended and unattended speech are different (O’Sullivan et al.,
603 2014, Ding & Simon 2012a), possibly reflecting distinct neural mechanisms related to
604 attending and suppressing the target and non-target speech streams, respectively. When
605 examining correlations to the non-target speech predicted by ‘attended’ models trained on
606 single-talker speech data, we observed an enhanced correlation in the HI listeners, both in
607 the forward ($t(41.87) = -2.28$, $p = 0.0276$) and backward model ($t(41.53) = -3.27$, $p =$
608 0.0022) correlations. The reason for this is unclear, but could for instance arise if listeners
609 momentarily switch their attention to the non-target speech, or, if the response functions

610 for attended and unattended speech are correlated, in which case a change in attended
611 response functions in HI listeners could affect the correlations between model predictions
612 and non-target speech.

613

614 [Insert Figure 4 about here]

615

616 ***Envelope entrainment to tones during passive stimulation***

617 The speech experiments with single and competing talkers both suggested an enhanced
618 envelope entrainment to attended speech in HI listeners, possibly indicating a stimulus-
619 driven effect. Next, we recorded responses to tone sequences during passive stimulation
620 to obtain measures of stimulus-driven cortical entrainment. We used periodic tone stimuli
621 designed to entrain steady-state cortical activity in the gamma (40 Hz) or theta (4 Hz)
622 range (stimuli illustrated in Fig. 5a). Specifically, periodic 4 Hz tone stimulation examines
623 envelope response entrainment in the frequency range also examined in the analysis of
624 the speech stimuli (< 10 Hz), but without the attention task component. We computed the
625 inter-trial phase coherence (ITPC) to assess how precisely EEG activity synchronized to
626 the periodic tone stimulation. We computed the ITPC in time windows of 0.5 s to
627 investigate potential differences in ITPC over the 2 s stimulation period. Figure 5b-d shows
628 the ITPC results for the two types of tone stimuli. For the 4 Hz stimulation (Fig. 5c, top
629 row), a repeated measures ANOVA on the ITPC revealed a main effect of hearing
630 impairment ($F(1,42) = 5.00, p = 0.0306$), a main effect of time ($F(3,126) = 85.18, p <$
631 0.0001) as well as an interaction effect ($F(3,126) = 5.68, p = 0.0011$). Post hoc t-tests
632 revealed that the 4 Hz ITPC was significantly higher (after applied FDR corrections, $q =$
633 0.05) for HI than for NH in the time period 0 s to 1 s post onset, but not in the later part of
634 the stimulation (0-0.5 s: $t(41.92) = -2.82, p = 0.0072$; 0.5-1.0 s: $t(41.44) = -2.78, p =$

635 0.0081; 1.0-1.5 s: $t(41.43) = -1.57, p = 0.1240$; 1.5-2.0 s: $t(41.92) = -0.93, p = 0.3583$). On
636 the other hand, the ITPC for 40 Hz stimulation (Fig. 5c, bottom row) showed no main effect
637 of hearing loss ($F(1,42) = 1.65, p = 0.2058$), or time ($F(3,126) = 1.36, p = 0.2572$). As
638 indicated in the topographies (Fig. 5d), the ITPC at both rates were prominent at fronto-
639 central electrodes and showed no lateralization effects.

640

641 [Insert Figure 5 about here]

642

643 ***ERP tone responses***

644

645 Enhanced envelope-following responses to tones or speech could potentially be driven by
646 an overall enhanced cortical reactivity to sound transients (Aiken & Picton, 2008) following
647 hearing loss. To test whether HI affects transient-evoked EEG responses (Alain et al.,
648 2014), we measured ERP responses to 1 kHz tone beeps presented with random inter-
649 onset intervals during passive listening. No effect of hearing impairment was found on the
650 mean amplitude of the N1 component ($t(41.97) = 0.83, p = 0.4092$). We also extracted
651 ERPs elicited by the individual tones in the periodic EFR tone stimuli discussed above.
652 Again, no effect of hearing impairment on the mean N1 amplitudes was observed, neither
653 for the 4 Hz ($t(40.07) = 0.015, p = 0.9883$) nor the 40 Hz EFR stimuli ($t(41.71) = 1.77, p =$
654 0.0847). This also indicates that observed changes in phase coherence of the EFR
655 responses with hearing loss are not driven by changes in the amplitude of transient
656 evoked activity (Van Diepen and Mazaheri 2018).

657

658 **Discussion**

659

660 Speech-in-noise listening difficulties are among the most severe consequences of
661 presbycusis, often persisting even when loss of audibility is accounted for, e.g. by a

662 hearing aid (Kochkin, 2005). Here, we investigated effects of sensorineural hearing loss on
663 cortical processing of competing speech. Behaviorally, questionnaire data (SSQ)
664 confirmed that HI listeners, compared to age-matched NH controls, experience
665 significantly greater listening difficulties in everyday noisy situations (while using their
666 hearing aid). This was mirrored by elevated speech reception thresholds in stationary
667 noise (Fig. 2b). Although elevated, SRTs for HI listeners remained negative for most
668 subjects. Conversational speech in daily life most often occurs at positive signal-to-noise
669 ratios (Olsen 1998; Billings and Madsen 2018) and rarely at noise levels where only half of
670 the speech can be recognized (i.e. 50% SRTs as considered here). In our EEG
671 experiments, we recorded EEG from subjects listening to competing speech signals
672 presented in scenarios with good speech recognition in both listener groups. Yet, listening
673 to speech with a competing talker was rated as being significantly more difficult for
674 listeners with hearing loss compared to NH controls (Fig. 1).

675

676 Previous work has associated hearing loss with weakened differential responses to
677 competing streams of tones (Dai et al., 2017) or speech (Petersen et al., 2016) in
678 challenging acoustic situations where hearing impairments are likely to affect sound
679 segregation abilities. Dai et al. (2017) found less differential ERP responses to target and
680 distractor tone streams in a spatial selective task where HI listeners performed poorer than
681 NH listeners. These results are consistent with the notion that cortical tracking operates on
682 segregated 'auditory objects' (Simon, 2015), whereby the inability to segregate objects (in
683 NH and HI listeners alike) reduces the differential tracking of competing streams (Kong et
684 al, 2015; Elhilali et al. 2009). In contrast to the present study, Petersen et al. (2016)
685 reported a weaker differential entrainment with increasing amounts of hearing loss in a

686 selective-listening task where HI and NH were matched in performance. This discrepancy
687 could relate to the fact that Petersen et al. (2016) used spatially co-located speech
688 streams at SRTs around 80% where segregation may be challenging. To achieve similar
689 speech performance, the level of the target speech relative to the masker speech was
690 increased with increasing amount of hearing loss, making it difficult to isolate effects of
691 attention from differences in target-to-masker ratios. It has thus been unclear whether
692 listeners with hearing loss would be able to engage selective attention to suppress
693 distracting speech in situations where the perceptual segregation of the distractor is not a
694 bottleneck on performance.

695

696 In the present study, we addressed this by using spatially separated speech streams
697 spoken by a male and female talker, providing both spatial cues and pitch cues for robust
698 segregation. Despite self-reported listening difficulties, cortical synchronization to speech
699 mixtures was found to be strongly modulated by attention in the HI listeners. Increased
700 difficulty suppressing distractor speech in the situation where the distractor can be
701 segregated could potentially have been associated with a less differential cortical
702 response to the attended and ignored streams, but this was not observed. Instead,
703 compared to age-matched NH controls, listeners with hearing loss showed (a) enhanced
704 low-frequency envelope-entrained cortical responses, both for the attended speech (Fig.
705 3) and 4 Hz modulated tone stimuli (Fig. 5), and (b) a robust effect of attention on the
706 cortical speech-entrained responses (Fig. 4). Such enhanced envelope representations
707 could contribute to perceptual difficulties, as suggested by previous work (Millman et al.,
708 2017). However, enhanced responses were not observed for the unattended speech. It is
709 possible that HI listeners with altered envelope processing have to rely on attention to an

710 even greater degree to suppress fluctuating distractor signals, and may be well-trained
711 trained to do so.

712

713 ***Mechanisms of amplified envelope coding?***

714 Increased envelope synchronization in the central auditory system following sensorineural
715 hearing loss concurs with previous results (Zhong et al., 2014; Goossens et al., 2018),
716 where the degree of enhancement has been associated with speech-in-noise deficits
717 (Millman et al., 2017; Goossens et al., 2018). This suggests that amplified envelope coding
718 in cortex may represent an upstream consequence of peripheral hearing damage that
719 might itself have detrimental effects for speech-in-noise perception (Carney, 2018). It is
720 known from speech psychophysics with NH listeners that artificially expanding the
721 envelope of a speech signal reduces speech intelligibility (e.g. Moore and Glasberg, 1993;
722 van Buuren et al., 1999). Envelope expansion in combination with simulated high-
723 frequency sloping hearing loss has only minor effects on the intelligibility of a single
724 speech signal when audibility is accounted for (e.g. by a hearing aid), but degrades the
725 intelligibility of a speech signal in the presence of other talkers (Moore and Glasberg,
726 1993).

727

728 Amplified envelope coding following hearing loss has been observed previously both in the
729 auditory periphery (Kale and Heinz, 2010) and at central stages of the auditory system
730 (Zhong et al., 2014; Millman et al., 2017; Heeringa and van Dijk, 2018; Goossens et al.,
731 2019). It is thus possible that effects observed in cortex could be inherited from the
732 periphery. In presbycusis, loss of outer hair cells reduces the fast-acting compressive
733 response of the basilar membrane in the cochlea (Ruggero and Rich, 1991). For mid- and

734 high-level sounds, this loss of compression leads to a steeper level-response function and
735 is considered to result in loudness recruitment (Moore and Oxenham, 1998). Kale and
736 Heinz (2010) showed that noise-induced sensorineural hearing loss enhances the
737 envelope synchrony of auditory nerve fiber responses, indicating that cochlear damage
738 can lead to an enhanced envelope coding at the level of the auditory nerve.

739

740 Enhanced envelope responses observed in cortex may, however, also reflect a
741 compensatory gain of reduced peripheral input at central auditory stages. Upregulated
742 activity in response to cochlear damage has been observed throughout the auditory
743 pathway (Gerken, 1979; Qiu et al., 2000; Mulders and Robertson, 2009; Sun et al., 2012;
744 Wei, 2013). Increased excitability of central neurons could help minimize sensitivity loss,
745 but could also lead to hyperactivity for mid- and high-level sounds (Hughes et al., 2010;
746 Salvi et al., 2017, Chambers et al., 2016). Potential homeostatic mechanisms underlying
747 such hyperactivity remain debated, but both cochlear damage and aging are known to
748 decrease GABA-mediated inhibitory neurotransmission in the auditory midbrain and cortex
749 (Caspary et al., 2008, 2013). While decreased inhibition may help maintain mean activity
750 levels (Turrigiano, 1999; Wang et al., 2002), it may at the same time degrade precise
751 frequency tuning (Wang et al., 2000, 2002; Barsz et al. 2007) and accurate spike timing
752 (Wehr and Zador, 2003; Xie 2016), potentially affecting cues that are important for
753 discrimination and segregation of sounds.

754

755 A number of studies have reported amplified envelope coding as an effect of aging
756 (Walton et al., 2002; Goossens et al., 2016; Presacco et al., 2016a, 2016b, 2019;
757 Herrmann et al., 2017, 2019; Parthasarathy et al., 2019) also in listeners with relatively

758 normal thresholds. Normal aging has been associated neural degeneration of auditory
759 nerve fibers (Sergeyenko et al., 2013; Wu et al., 2019), which has also been associated
760 with hyper-excitability in the central auditory system (Herrmann et al., 2017, 2019;
761 Parthasarathy et al., 2019). Such cochlear neuropathy can occur without hair cell damage
762 (Viana et al., 2015) and is likely to be further advanced in older listeners with clinical
763 threshold shifts.

764

765 **Caveats**

766 In our experiments, the speech stimuli were amplified to minimize effects of differences in
767 audibility. This was done to examine potential effects of attention-driven speech
768 processing in situations where the speech stimulus is audible. Frequency-dependent
769 amplification based on the audiogram mirrors the situation of aided listening (e.g. with a
770 linear hearing aid), where HI listeners experience difficulties in competing-talker situations
771 (e.g. Fig. 2c). We note that matching hearing level based on the audiogram may not
772 necessarily match the peripheral activation level and potential effects of amplification of
773 the overall level on EEG correlates of envelope coding are undetermined.

774

775 **BCI Perspectives**

776 Finally, we note that the current results may have relevance for auditory brain-computer
777 interfaces. In combination with speech audio separation technologies, single-trial EEG
778 decoding of attention could be used to amplify an attended speech stream in a neuro-
779 steered hearing instrument to help ease listening difficulties in multi-talker situations
780 (O'Sullivan et al., 2017; Mirkovic et al., 2016). Although enhanced cortical representations
781 of speech envelopes may not be beneficial to speech perception, they did not hinder

782 decoding of selective auditory attention from single-trial EEG responses in older listeners
783 with hearing loss. However, it is not clear yet how robust attention decoding would be in
784 less favorable SNRs in HI listeners.

785

786

787

788 **References**

789

790 Aiken SJ, Picton TW (2008) Human cortical responses to the speech envelope. *Ear Hear*
791 29:139–157.

792 Akeroyd MA (2008) Are individual differences in speech reception related to individual
793 differences in cognitive ability? A survey of twenty experimental studies with normal
794 and hearing-impaired adults. *Int J Audiol* 47:S53--S71.

795 Alain C, Roye A, Salloum C (2014) Effects of age-related hearing loss and background
796 noise on neuromagnetic activity from auditory cortex. *Front Syst Neurosci* 8:8.

797 Andrés P, Parmentier FBR, Escera C (2006) The effect of age on involuntary capture of
798 attention by irrelevant sounds: a test of the frontal hypothesis of aging.
799 *Neuropsychologia* 44:2564–2568.

800 Barsz, K, Wilson, WW, & Walton, JP (2007). Reorganization of receptive fields following
801 hearing loss in inferior colliculus neurons. *Neuroscience*, 147:532-545.

802 Benjamini Y, Hochberg Y (1995) Controlling the false discovery rate: a practical and
803 powerful approach to multiple testing. *J R Stat Soc Ser B*, 57:289–300.

804 Billings CJ, Madsen BM (2018) A perspective on brain-behavior relationships and effects
805 of age and hearing using speech-in-noise stimuli. *Hear Res* 369:90-102

806 Bisgaard N, Vlaming MSMG, Dahlquist M (2010) Standard audiograms for the IEC 60118-
807 15 measurement procedure. *Trends Amplif* 14:113–120.

808 Blackburn HL, Benton AL (1957) Revised administration and scoring of the digit span test.
809 *J Consult Psychol* 21:139.

810 Carney LH (2018) Supra-Threshold Hearing and Fluctuation Profiles: Implications for
811 Sensorineural and Hidden Hearing Loss. *JARO - J Assoc Res Otolaryngol* 19:331–
812 352.

- 813 Caspary DM, Hughes LF, Ling LL (2013) Age-related GABAA receptor changes in rat
814 auditory cortex. *Neurobiol Aging* 34:1486–1496.
- 815 Caspary DM, Ling L, Turner JG, Hughes LF (2008) Inhibitory neurotransmission, plasticity
816 and aging in the mammalian central auditory system. *J Exp Biol* 211:1781–1791.
- 817 Chambers AR, Resnik J, Yuan Y, Whitton JP, Edge AS, Liberman MC, Polley DB (2016)
818 Central Gain Restores Auditory Processing following Near-Complete Cochlear
819 Denervation. *Neuron* 89:867–879
- 820 Dai L, Best V, Shinn-Cunningham BG (2018) Sensorineural hearing loss degrades
821 behavioral and physiological measures of human spatial selective auditory attention.
822 *Proc Natl Acad Sci*:201721226
- 823 De Cheveigné A, Parra LC (2014) Joint decorrelation, a versatile tool for multichannel data
824 analysis. *Neuroimage* 98:487–505.
- 825 Di Liberto GM, O'Sullivan JA, Lalor EC (2015) Low-frequency cortical entrainment to
826 speech reflects phoneme-level processing. *Curr Biol* 25:2457–2465.
- 827 Ding N, Simon JZ (2012a) Neural coding of continuous speech in auditory cortex during
828 monaural and dichotic listening. *J Neurophysiol* 107:78–89.
- 829 Ding N, Simon JZ (2012b) Emergence of neural encoding of auditory objects while
830 listening to competing speakers. *Proc Natl Acad Sci* 109:11854–11859.
- 831 Ding N, Simon JZ (2013) Adaptive temporal encoding leads to a background-insensitive
832 cortical representation of speech. *J Neurosci* 33:5728–5735.
- 833 Ding N, Simon JZ (2014) Cortical entrainment to continuous speech: functional roles and
834 interpretations. *Front Hum Neurosci* 8:1–7.
- 835 Dubno JR, Horwitz AR, Ahlstrom JB (2002) Benefit of modulated maskers for speech
836 recognition by younger and older adults with normal hearing. *J Acoust Soc Am*

- 837 111:2897–2907.
- 838 Elhilali, M, Xiang, J, Shamma, SA, & Simon, JZ (2009). Interaction between attention and
839 bottom-up saliency mediates the representation of foreground and background in an
840 auditory scene. *PLoS Biol* 7:e1000129.
- 841 Gatehouse S, Noble W (2004) The speech, spatial and qualities of hearing scale (SSQ).
842 *Int J Audiol* 43:85–99.
- 843 Gazzaley A, Clapp W, Kelley J, McEvoy K, Knight RT, D’Esposito M (2008) Age-related
844 top-down suppression deficit in the early stages of cortical visual memory processing.
845 *Proc Natl Acad Sci* 105:13122–13126.
- 846 Gazzaley A, Cooney JW, Rissman J, D’Esposito M (2005) Top-down suppression deficit
847 underlies working memory impairment in normal aging. *Nat Neurosci* 8:1298.
- 848 Gerken GM (1979) Central denervation hypersensitivity in the auditory system of the cat. *J*
849 *Acoust Soc Am* 66:721–727.
- 850 Glasberg BR, Moore BCJ (1990) Derivation of auditory filter shapes from notched-noise
851 data. *Hear Res* 47:103–138.
- 852 Golumbic EMZ, Ding N, Bickel S, Lakatos P, Schevon CA, McKhann GM, Goodman RR,
853 Emerson R, Mehta AD, Simon JZ, others (2013) Mechanisms underlying selective
854 neuronal tracking of attended speech at a “cocktail party.” *Neuron* 77:980–991.
- 855 Goossens T, Vercammen C, Wouters J, van Wieringen A (2018) Neural envelope
856 encoding predicts speech perception performance for normal-hearing and hearing-
857 impaired adults. *Hear Res* 370:189-200.
- 858 Goossens T, Vercammen C, Wouters J, van Wieringen A (2019) The association between
859 hearing impairment and neural envelope encoding at different ages. *Neurobiol Aging*
860 74:202–212.

- 861 Goossens T, Vercammen C, Wouters J, Wieringen A van (2016) Aging affects neural
862 synchronization to speech-related acoustic modulations. *Front Aging Neurosci* 8:133.
- 863 Grimault N, Micheyl C, Carlyon RP, Arthaud P, Collet L (2001) Perceptual auditory stream
864 segregation of sequences of complex sounds in subjects with normal and impaired
865 hearing. *Br J Audiol* 35:173–182.
- 866 Heeringa AN, van Dijk P (2018) Neural coding of the sound envelope is changed in the
867 inferior colliculus immediately following acoustic trauma. *Eur J Neurosci* 49:1220-
868 1232.
- 869 Herrmann, B, Buckland, C, & Johnsrude, IS (2019). Neural signatures of temporal
870 regularity processing in sounds differ between younger and older adults. *Neurobiol*
871 *Aging*, 83:73-85.
- 872 Herrmann B, Parthasarathy A, Bartlett EL (2017) Ageing affects dual encoding of
873 periodicity and envelope shape in rat inferior colliculus neurons. *Eur J Neurosci*
874 45:299–311.
- 875 Hughes LF, Turner JG, Parrish JL, Caspary DM (2010) Processing of broadband stimuli
876 across A1 layers in young and aged rats. *Hear Res* 264:79–85.
- 877 Kale S, Heinz MG (2010) Envelope coding in auditory nerve fibers following noise-induced
878 hearing loss. *JARO - J Assoc Res Otolaryngol* 11:657–673.
- 879 Kochkin S (2005) MarkeTrak VII: Customer satisfaction with hearing instruments in the
880 digital age. *Hear J* 58:30–32.
- 881 Kong, YY, Somarowthu, A, Ding, N (2015). Effects of spectral degradation on attentional
882 modulation of cortical auditory responses to continuous speech. *J Assoc Res*
883 *Otolaryngol* 16:783-796.
- 884 Larsby B, Arlinger S (1999) Auditory Temporal and Spectral Resolution in Normal and

- 885 Impaired Hearing. *J Am Acad Audiol* 10:198–210.
- 886 Luo H, Poeppel D (2007) Phase patterns of neuronal responses reliably discriminate
887 speech in human auditory cortex. *Neuron* 54:1001–1010.
- 888 Millman RE, Mattys SL, Gouws AD, Prendergast G (2017) Magnified Neural Envelope
889 Coding Predicts Deficits in Speech Perception in Noise. *J Neurosci* 37:7727–7736.
- 890 Mirkovic B, Bleichner MG, De Vos M, Debener S (2016) Target speaker detection with
891 concealed {EEG} around the ear. *Front Neurosci* 10:349.
- 892 Mirkovic B, Debener S, Jaeger M, De Vos M (2015) Decoding the attended speech stream
893 with multi-channel EEG: implications for online, daily-life applications. *J Neural Eng*
894 12:46007.
- 895 Moore BCJ (1986) *Frequency selectivity in hearing*. Academic Press.
- 896 Moore BCJ, Glasberg BR (1993) Simulation of the effects of loudness recruitment and
897 threshold elevation on the intelligibility of speech in quiet and in a background of
898 speech. *J Acoust Soc Am* 94:2050–2062.
- 899 Moore BCJ, Glasberg BR (1998) Use of a loudness model for hearing-aid fitting. I. Linear
900 hearing aids. *Br J Audiol* 32:317–335.
- 901 Moore BCJ, Glasberg BR, Vickers DA (1995) Simulation of the effects of loudness
902 recruitment on the intelligibility of speech in noise. *Br J Audiol* 29:131–143.
- 903 Moore BCJ, Oxenham AJ (1998) Psychoacoustic consequences of compression in the
904 peripheral auditory system. *Psychol Rev* 105:108.
- 905 Morel P (2016) *Gramm: grammar of graphics plotting in Matlab*.
- 906 Mulders W, Robertson D (2009) Hyperactivity in the auditory midbrain after acoustic
907 trauma: dependence on cochlear activity. *Neuroscience* 164:733–746.
- 908 Nielsen JB, Dau T (2009) Development of a Danish speech intelligibility test. *Int J Audiol*

- 909 48:729–741.
- 910 O’Sullivan JA, Chen Z, Herrero J, McKhann GM, Sheth SA, Mehta AD, Mesgarani N
911 (2017) Neural decoding of attentional selection in multi-speaker environments without
912 access to clean sources. *J Neural Eng* 14:56001.
- 913 O’Sullivan JA, Power AJ, Mesgarani N, Rajaram S, Foxe JJ, Shinn-Cunningham BG,
914 Slaney M, Shamma SA, Lalor EC (2014) Attentional selection in a cocktail party
915 environment can be decoded from single-trial EEG. *Cereb Cortex* 25:1697–1706.
- 916 Oostenveld R, Fries P, Maris E, Schoffelen J-M (2011) FieldTrip: open source software for
917 advanced analysis of MEG, EEG, and invasive electrophysiological data. *Comput
918 Intell Neurosci* 2011:1.
- 919 Oreinos C, Buchholz JM (2013) Measurement of a full 3D set of HRTFs for in-ear and
920 hearing aid microphones on a head and torso simulator (HATS). *Acta Acust united
921 with Acust* 99:836–844.
- 922 Parthasarathy A, Herrmann B, Bartlett EL (2019) Aging alters envelope representations of
923 speech-like sounds in the inferior colliculus. *Neurobiol Aging* 73:30–40.
- 924 Peelle JE, Wingfield A (2016) The Neural Consequences of Age-Related Hearing Loss.
925 *Trends Neurosci* 39:486–497.
- 926 Petersen EB, Wöstmann M, Obleser J, Lunner T (2017) Neural tracking of attended versus
927 ignored speech is differentially affected by hearing loss. *J Neurophysiol* 117:18–27.
- 928 Presacco A, Simon JZ, Anderson S (2016a) Evidence of degraded representation of
929 speech in noise, in the aging midbrain and cortex. *J Neurophysiol* 116:2346–2355.
- 930 Presacco A, Simon JZ, Anderson S (2016b) Effect of informational content of noise on
931 speech representation in the aging midbrain and cortex. *J Neurophysiol* 116:2356–
932 2367.

- 933 Presacco A, Simon JZ, Anderson S (2019) Speech-in-noise representation in the aging
934 midbrain and cortex: Effects of hearing loss. *PLoS One* 14:e0213899.
- 935 Prichard D, Theiler J (1994) Generating surrogate data for time series with several
936 simultaneously measured variables. *Phys Rev Lett* 73:951.
- 937 Qiu CX, Salvi R, Ding D, Burkard R (2000) Inner hair cell loss leads to enhanced response
938 amplitudes in auditory cortex of unanesthetized chinchillas: Evidence for increased
939 system gain. *Hear Res* 139:153–171.
- 940 Rajan R, Cainer KE (2008) Ageing without hearing loss or cognitive impairment causes a
941 decrease in speech intelligibility only in informational maskers. *Neuroscience*
942 154:784–795.
- 943 Rousselet GA (2012) Does filtering preclude us from studying ERP time-courses? *Front*
944 *Psychol* 3:1–9.
- 945 Ruggero MA, Rich NC (1991) Furosemide alters organ of Corti mechanics: evidence for
946 feedback of outer hair cells upon the basilar membrane. *J Neurosci* 11:1057–1067.
- 947 Salvi R, Sun W, Ding D, Chen G-D, Lobarinas E, Wang J, Radziwon K, Auerbach BD
948 (2017) Inner hair cell loss disrupts hearing and cochlear function leading to sensory
949 deprivation and enhanced central auditory gain. *Front Neurosci* 10:621.
- 950 Schoof T, Rosen S (2014) The role of auditory and cognitive factors in understanding
951 speech in noise by normal-hearing older listeners. *Front Aging Neurosci* 6:1–14.
- 952 Sergeyenko Y, Lall K, Liberman MC, Kujawa SG (2013) Age-related cochlear
953 synaptopathy: an early-onset contributor to auditory functional decline. *J Neurosci*
954 33:13686–13694.
- 955 Shinn-Cunningham BG, Best V (2008) Selective attention in normal and impaired hearing.
956 *Trends Amplif* 12:283–299.

- 957 Simon, JZ (2015). The encoding of auditory objects in auditory cortex: insights from
958 magnetoencephalography. *Int J Psychophysiol* 95:184-190.
- 959 Søndergaard PL, Majdak P (2013) The auditory modeling toolbox. In: *The technology of*
960 *binaural listening*, pp 33–56. Springer.
- 961 Sun W, Deng A, Jayaram A, Gibson B (2012) Noise exposure enhances auditory cortex
962 responses related to hyperacusis behavior. *Brain Res* 1485:108–116.
- 963 Turrigiano GG (1999) Homeostatic plasticity in neuronal networks: the more things
964 change, the more they stay the same. *Trends Neurosci* 22:221–227.
- 965 van Buuren RA, Festen JM, Houtgast T (1999) Compression and expansion of the
966 temporal envelope: Evaluation of speech intelligibility and sound quality. *J Acoust Soc*
967 *Am* 105:2903–2913.
- 968 van Diepen, RM, Mazaheri, A (2018) The caveats of observing inter-trial phase-coherence
969 in cognitive neuroscience. *Sci Rep*, 8:2990.
- 970 Van Gerven PWM, Guerreiro MJS (2016) Selective attention and sensory modality in
971 aging: curses and blessings. *Front Hum Neurosci* 10:147.
- 972 VanRullen R (2011) Four common conceptual fallacies in mapping the time course of
973 recognition. *Front Psychol* 2:1–6.
- 974 Viana LM, O'Malley JT, Burgess BJ, Jones DD, Oliveira CACP, Santos F, Merchant SN,
975 Liberman LD, Liberman MC (2015) Cochlear neuropathy in human presbycusis:
976 Confocal analysis of hidden hearing loss in post-mortem tissue. *Hear Res* 327:78–88.
- 977 Walton JP, Simon H, Frisina RD (2002) Age-Related Alterations in the Neural Coding of
978 Envelope Periodicities. *J Neurophysiol* 88:565–578.
- 979 Wang J, Caspary D, Salvi RJ (2000) GABA-A antagonist causes dramatic expansion of
980 tuning in primary auditory cortex. *Neuroreport* 11:1137–1140.

- 981 Wang J, McFadden SL, Caspary D, Salvi R (2002) Gamma-aminobutyric acid circuits
982 shape response properties of auditory cortex neurons. *Brain Res* 944:219–231.
- 983 Wehr M, Zador AM (2003) Balanced inhibition underlies tuning and sharpens spike timing
984 in auditory cortex. *Nature* 426:442.
- 985 Wei S (2013) Peripheral hearing loss causes hyperexcitability of the inferior colliculus. *J*
986 *Otol* 8:39–43.
- 987 Wingfield A, Peelle JE (2012) How does hearing loss affect the brain? *Aging health* 8:107–
988 109.
- 989 Wingfield A, Tun PA (2001) Spoken language comprehension in older adults: Interactions
990 between sensory and cognitive change in normal aging. In: *Seminars in Hearing*, pp
991 287–302.
- 992 Wong DDE, Fuglsang SA, Hjortkjær J, Ceolini E, Slaney M, de Cheveigné A (2018) A
993 comparison of regularization methods in forward and backward models for auditory
994 attention decoding. *Front Neurosci* 12:531.
- 995 Wu PZ, Liberman LD, Bennett K, De Gruttola V, O'Malley JT, Liberman MC (2019)
996 Primary neural degeneration in the human cochlea: evidence for hidden hearing loss
997 in the aging ear. *Neuroscience* 407:8–20.
- 998 Zhong Z, Henry KS, Heinz MG (2014) Sensorineural hearing loss amplifies neural coding
999 of envelope information in the central auditory system of chinchillas. *Hear Res*
1000 309:55–62.
- 1001 Xie, R (2016). Transmission of auditory sensory information decreases in rate and
1002 temporal precision at the endbulb of Held synapse during age-related hearing
1003 loss. *Journal of neurophysiology*, 116:2695-2705.
- 1004

1006 **Figure Legends**

1007

1008 **FIGURE 1.** Auditory attention EEG experiment. **a**, Schematic illustration of the trial
1009 sequences. EEG data were recorded from subjects selectively listening to audiobooks
1010 narrated by a male and a female speaker. After each trial, the subjects were asked to rate
1011 task difficulty and respond to multiple-choice questions related to the content of the
1012 attended speech stream. **b**, Behavioral results from the selective auditory attention
1013 experiment showing difficulty rating scores (left) comprehension scores (right). Error bars
1014 indicate s.e.m.

1015

1016 **FIGURE 2.** Behavioral hearing tests. **a**, Pure-tone audiograms for the normal-hearing
1017 (upper panel) and hearing-impaired (lower panel) subjects. Each thin line represents the
1018 audiogram for a single subject averaged over both ears. The thick lines represent
1019 averages across subjects. **b**, Sentence reception thresholds (SRT) in the two groups
1020 measured in a speech-in-noise recognition task. **c**, Self-assessed hearing disabilities as
1021 assessed by the Speech, Spatial and Qualities of Hearing Scale questionnaire (SSQ).
1022 Lower ratings indicate greater self-rated listening difficulties in everyday acoustic
1023 environments. The SSQ scores shown here are averaged over three SSQ subsections
1024 ("speech", "qualities" and "spatial"). **d**, Tone detection in noise with or without a 50 ms
1025 temporal gap. Hearing-impaired listeners showed less temporal release of masking (RoM),
1026 i.e. they showed a smaller benefit from temporal gaps in the noise masker compared to
1027 normal hearing listeners. **e**, Working memory performance as measured by a backwards
1028 digit span test.

1029

1030 **FIGURE 3.** Results from the encoding analysis. **Left:** Group mean encoding accuracies
1031 averaged over fronto-central electrodes. Encoding accuracies indicate the correlation
1032 between speech envelope model predictions and EEG data from normal-hearing (light
1033 blue) and hearing-impaired (dark blue) listeners. Each point represents data from a single
1034 subject. Error bars represent s.e.m. The shaded area indicates the estimated noise floor.

1035 **Right:** Topographies showing group-mean encoding accuracies at each electrode site.

1036

1037 **FIGURE 4.** Results of the attention decoding analysis. Stimulus reconstruction models
1038 trained on EEG responses to single-talker speech stimuli were used to decode the
1039 attended target from 10 s long EEG responses to two-talker stimuli. For a given test
1040 segment, correct classification indicates that the correlation with the speech envelope of
1041 the attended stream r_{attended} was higher than the unattended $r_{\text{unattended}}$. **Left:** Attention

1042 classification accuracies in normal hearing and hearing-impaired listeners. Each point
1043 represents data averaged from a single subject. The dashed line represents chance-level.

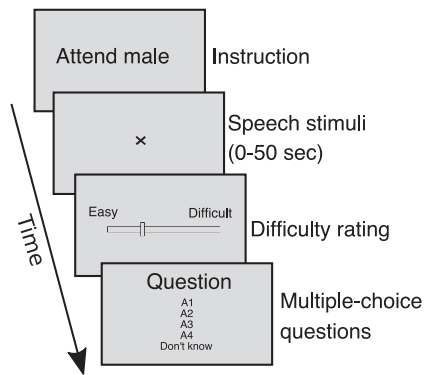
1044 Error bars indicate s.e.m. **Right:** Single-trial reconstruction accuracies for each 10 s long
1045 decoding segment. Each point reflects accuracies for a given subject and a given
1046 decoding segment. Data is here shown for all subjects and all 10 s decoding segments.

1047

1048 **FIGURE 5.** EFR responses to periodic tone sequences during passive stimulation. Top
1049 row shows EFR stimuli and responses to 0.25 s on/off segments of 40 Hz tone stimuli.
1050 Bottom row shows stimuli and responses to 2 s long 40 Hz tone stimuli. **a,** EFR tone
1051 stimuli. **b,** Time-frequency representations of inter-trial phase coherence (ITPC) for
1052 normal-hearing (NH, left) and hearing-impaired (HI, right) listeners for the two types of
1053 stimuli. **c,** ITPC averaged over all scalp electrodes for NH and HI listeners, in

1054 nonoverlapping 0.5 s long time intervals. Shaded areas indicate s.e.m. The individual red
1055 (HI) and blue (NH) points represent data from each subject. **d**, Topographies of group-
1056 mean ITPC at each electrode in the stimulation period (0-2 s).
1057

a Selective auditory attention experiment



b Behavioural results from selective auditory attention experiment

